BIOCHEMISTRY
including biophysical chemistry & molecular biology

Article

Characterization of Dehaloperoxidase Compound ES and Its Reactivity with Trihalophenols

Jeremiah Feducia, Rania Dumarieh, Lauren B. G. Gilvey, Tatyana Smirnova, Stefan Franzen, and Reza A. Ghiladi

Biochemistry, **2009**, 48 (5), 995-1005• DOI: 10.1021/bi801916j • Publication Date (Web): 15 January 2009

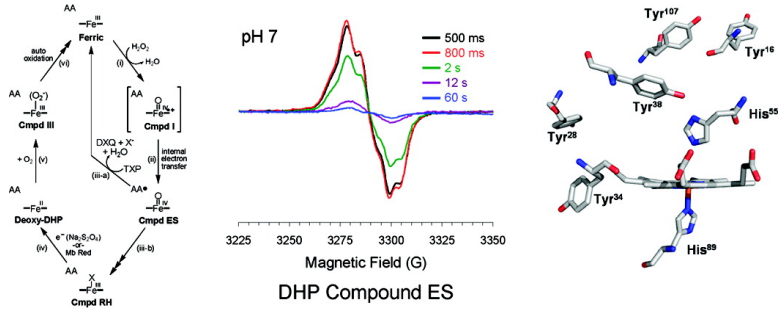

More About This Article

Additional resources and features associated with this article are available within the HTML version:

- Supporting Information
- Access to high resolution figures
- Links to articles and content related to this article
- Copyright permission to reproduce figures and/or text from this article

View the Full Text HTML

Characterization of Dehaloperoxidase Compound ES and Its Reactivity with Trihalophenols[†]

Jeremiah Feducia, Rania Dumarieh, Lauren B. G. Gilvey, Tatyana Smirnova, Stefan Franzen,* and Reza A. Ghiladi*

Department of Chemistry, North Carolina State University, Raleigh, North Carolina 27695

Received October 12, 2008; Revised Manuscript Received November 18, 2008

ABSTRACT: Dehaloperoxidase (DHP), the oxygen transport hemoglobin from the terebellid polychaete *Amphitrite ornata*, is the first globin identified to possess a biologically relevant peroxidase activity. DHP has been shown to oxidize trihalophenols to dihaloquinones in a dehalogenation reaction that uses hydrogen peroxide as a substrate. Herein, we demonstrate that the first detectable intermediate following the addition of hydrogen peroxide to ferric DHP contains both a ferryl heme and a tyrosyl radical, analogous to Compound ES of cytochrome *c* peroxidase. Furthermore, we provide a detailed kinetic description for the reaction of preformed DHP Compound ES with the substrate 2,4,6-trichlorophenol and demonstrate the catalytic competency of this intermediate in generating the product 2,4-dichloroquinone. Using rapid-freeze-quench electron paramagnetic resonance spectroscopy, we detected a $g \approx 2.0058$ signal confirming the presence of a protein radical in DHP Compound ES. In the absence of substrate, DHP Compound ES evolves to a new species, Compound RH, which is functionally unique to dehaloperoxidase. We propose that this intermediate plays a protective role against heme bleaching. While unreactive toward further oxidation, Compound RH can be reduced and subsequently bind dioxygen, generating oxyferrous DHP, which may represent the catalytic link between peroxidase and oxygen transport activities in this bifunctional protein.

The terebellid polychaete *Amphitrite ornata* contains an abundant coelomic hemoglobin (*1*) that has been named dehaloperoxidase (DHP)[1] (*2*). In the presence of hydrogen peroxide, this globin catalyzes the two-electron oxidation of a trihalophenol substrate to yield a dihaloquinone (Scheme 1). Although DHP is dependent upon the pH and substrate employed, kinetic assays demonstrate that DHP is 1−2 orders of magnitude faster than myoglobin (Mb) in its ability to dehalogenate substrate (*3*), and only 1 order of magnitude slower than horseradish peroxidase (HRP) (*4*). Thus, DHP is an anomaly: it functions as the oxygen transport protein in *A. ornata* despite having a low degree of sequence homology with other hemoglobins (*5*−*8*) yet exhibits significant peroxidase activity approaching that of HRP even though it possesses neither structural nor sequence homology with any known peroxidase.

Scheme 1: Reaction of DHP with Trihalogenated Phenolate and Hydrogen Peroxide Yields Quinone Products

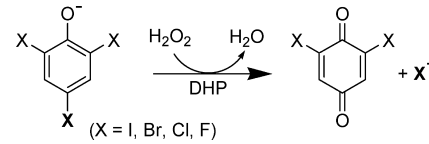

Despite a number of studies on DHP, how this bifunctional protein can act as both a hemoglobin and a peroxidase is still not understood (*1, 2, 4*). Peroxidases generally function via the Poulos−Kraut mechanism (*9*) in which H_2O_2 reacts with a ferric heme to form Compound I, the iron(IV)−oxo porphyrin π-cation radical species that is formally oxidized by two electrons relative to the ferric resting state. The majority of peroxidases regenerate the resting form of the enzyme via two sequential one-electron substrate oxidations ($2AH + H_2O_2 \rightarrow 2A^{\bullet} + 2H_2O$), proceeding through Compound II, an iron(IV)−oxo species that is one-electron-oxidized when compared to the ferric state. Furthermore, DHP (and HRP) has been shown to perform the net two-electron oxidation of phenols ($X-A-OH + H_2O_2 \rightarrow O=A=O + HX + H_2O$) to yield the corresponding quinones, again consistent with the formation of a two-electron-oxidized intermediate (*10*−*12*). However, the reaction of

[†] This project was supported by Army Research Office Grant 52278-LS.

* To whom correspondence should be addressed. S.F.: Department of Chemistry, North Carolina State University, Raleigh, NC 27695; phone, (919) 515-8915; fax, (919) 515-8920; e-mail, Stefan_Franzen@ncsu.edu. R.A.G.: Department of Chemistry, North Carolina State University, Raleigh, NC 27695; phone, (919) 513-0680; fax, (919) 515-8920; e-mail, Reza_Ghiladi@ncsu.edu.

[1] Abbreviations: DHP, dehaloperoxidase; Hb, hemoglobin; HRP, horseradish peroxidase; Mb, myoglobin; 4IP, 4-iodophenol; 4BP, 4-bromophenol; DCP, 2,4-dichlorophenol; TBP, 2,4,6-tribromophenol; TCP, 2,4,6-trichlorophenol; TFP, 2,4,6-trifluorophenol; TXP, trihalophenol; DXQ, dihalophenol; RFQ-CW-EPR, rapid-freeze-quench continuous wave electron paramagnetic resonance; Compound I, two-electron-oxidized heme center when compared to the ferric form, commonly as an $Fe^{IV}=O$ porphyrin π-cation radical; Compound II, one-electron-oxidized heme center when compared to the ferric form, commonly as an $Fe^{IV}=O$ or $Fe^{IV}-OH$; Compound III, oxyferrous [$Fe^{II}-O_2$ or $Fe^{III}-(O_2^-)$] state of the enzyme; Compound ES, two-electron-oxidized state containing both a ferryl center ($Fe^{IV}=O$) and an amino acid (tryptophanyl or tyrosyl) radical, analogous to Compound ES in cytochrome *c* peroxidase; Compound RH, "reversible heme" state of dehaloperoxidase, formed from the decay of Compound ES in the absence of substrate.

10.1021/bi801916j CCC: $40.75
Published on Web 01/15/2009

DHP with its physiological oxidant, H_2O_2, yields what has been characterized to date as Compound II (*7*), which is formally a one-electron-oxidized heme center. Thus, the question of how DHP oxidizes its phenol substrates by two electrons when it appears to form only a one-electron oxidized intermediate needs to be addressed.

Several possible mechanisms for a net two-electron oxidation exist, including the simplest notion that two sequential one-electron oxidations are required for DHP to oxidize a trihalophenol, the first generating a trihalophenoxy radical intermediate and the second yielding a trihalocyclohexanedienone cation which reacts with a solvent water molecule to yield the dihaloquinone product. These intermediates have been proposed by Osborne et al. to form during the oxidation of trichlorophenol to dichloroquinone by horse heart myoglobin (*3*). Another option is that DHP oxidizes trihalophenols by only one electron, forming a trihalophenoxy radical intermediate, which can undergo disproportionation with a second radical species, giving both trihalophenol and dihaloquinone. This proposed mechanism is reminiscent of ascorbate peroxidase (APX), which has been shown to oxidize ascorbate via a one-electron process to monohydroascorbate, the latter undergoing disproportionation to yield ascorbate and dehydroascorbate (*13*). A third possibility is that the intermediate in DHP formed from the reaction of the ferric enzyme with hydrogen peroxide is electronically similar to that of Compound ES in CcP, which has been shown to be isoelectronic with Compound I but in addition to the ferryl moiety also possesses a protein radical as the second oxidizing equivalent rather than a porphyrin-based one. This may be the favored mechanism, as it would allow for product formation via either (i) a direct two-electron oxidation (direct formation of the trihalocyclohexanedienone cation) without generating radical intermediates (which could be potentially harmful if formed in the coelom of *A. ornata*) or (ii) two sequential one-electron oxidations via a transiently formed trihalophenoxy radical that would be further oxidized to the dienone cation (*3*), potentially without first diffusing out of the active site pocket.

To explore mechanistic hypotheses, we have undertaken a comprehensive UV−visible and electron paramagnetic spectroscopic study of the DHP intermediate formed from the reaction of the ferric enzyme with hydrogen peroxide under a variety of conditions using both stopped-flow and rapid-freeze-quench methods and have determined this intermediate to be DHP Compound ES. We have further explored the stability of this Compound ES and demonstrated the existence of a competitive pathway between product formation and decay to a novel species, termed Compound RH, which possesses attenuated levels of dehaloperoxidase activity. Our experimental design reveals mechanistic insights and kinetic descriptions of the intermediates in DHP, which have not been previously reported. We propose an updated catalytic cycle which provides a clearer understanding of the link between peroxidase and oxygen transport activities unique to this bifunctional enzyme.

MATERIALS AND METHODS

Buffer salts and acetonitrile (HPLC-grade) were purchased from Fisher Scientific. All other reagents and biochemicals, unless otherwise specified, were of the highest grade available from Sigma-Aldrich. Solutions of 2,4,6-trichlorophenol (TCP) were freshly prepared daily in 100 mM potassium phosphate (KP_i) buffer (variable pH) and kept at 4 °C. UV−visible spectra were recorded periodically to ensure that the TCP substrate had not degraded (molar absorptivity listed in Table S1 of the Supporting Information). Hydrogen peroxide solutions were also freshly made prior to each experiment. Initially, a 10 mM stock solution of H_2O_2 was prepared and maintained at 4 °C (typically less than 15 min), during which all other protein/substrate solutions were loaded into the stopped-flow apparatus. When prepared in this manner, the stock H_2O_2 solution did not exhibit any degradation over this time period as determined by UV−visible spectroscopic analysis of the hydrogen peroxide absorbance at 240 nm ($\varepsilon_{240} = 43.6\ M^{-1}\ cm^{-1}$) (*18*). The stock H_2O_2 solution was then diluted to the appropriate premixing concentration and immediately loaded into the stopped-flow apparatus. Wild-type (WT) DHP (six-His-tagged protein) expression and purification procedures were preformed as previously described (*4*). TCP (4.05 mM maximum solubility) (*14*) was employed throughout this study due to the low solubility (0.355 mM) of TBP in aqueous solution (*15*).

Spectroscopic Studies. Optical spectra were recorded on either an Agilent 8453 diode array spectrophotometer or a Cary 50 UV−visible spectrophotometer, both equipped with thermostated cell holders at 25 °C. The protoheme content was measured by the pyridine hemochrome assay using a $\Delta\varepsilon_{557}$ of 20.7 $mM^{-1}\ cm^{-1}$ (reduced − oxidized) for iron protoporphyrin IX (*16, 17*).

Enzyme Assays. All measurements were performed in octiplet using a SpectraMax Plus384 UV−visible plate reader equipped with 96-well plates. Assays were carried out at 25 °C in 100 mM KP_i buffer (pH 7.5) containing 5 μM EDTA (total volume of 200 μL). Catalase activity was measured spectrophotometrically by following the decrease over 60 s (linear least-squares fittings) of the hydrogen peroxide concentration (1.5, 30, and 60 mM) at 240 nm ($\varepsilon_{240} = 43.6\ M^{-1}\ cm^{-1}$), in the presence of 1 μM DHP (*18*).

Preparation of Ferric DHP. DHP was incubated with a 1.7-fold molar excess of potassium ferricyanide for 2 min at room temperature. Excess ferricyanide was removed using a Sephadex G-25 gel-filtration column. The protein was concentrated using an Amicon Ultra centrifugal filter equipped with a 10000 kDa molecular mass membrane, and the purity of DHP was determined as previously described (*4*). Only DHP samples that exhibited Reinheitzahl values (RZ) greater than 4.0 were utilized in this study. The concentration of DHP was determined spectrophotometrically ($\varepsilon_{406} = 116.4\ mM^{-1}\ cm^{-1}$) (*19*).

Stopped-Flow UV−Visible Spectrophotometric Studies. Experiments were performed on a Bio-Logic SFM-400 triple-mixing stopped-flow instrument equipped with a diode array UV−visible spectrophotometer and were carried out at 20 °C in 100 mM KP_i buffer (pH 5.0 and 7.0). A constant temperature was maintained using a circulating water bath. Data were collected (900 scans total) over a three-time domain regime (2.5, 25, and 250 ms; 300 scans each) using Bio Kinet32 (Bio-Logic). Experiments were performed in double-mixing mode using an aging line prior to the second mixing step. The design of the experiments allowed for the mixing of DHP with either TCP or H_2O_2 followed by an aging time of 1.5, 30, or 60 s, followed by the second mix

with the remaining (co-) substrate: (i) DHP + TCP → delay → + H_2O_2 or (ii) DHP + H_2O_2 → delay → + TCP. Concentrations after mixing were as follows: $[DHP]_f = 10$ μM, $[H_2O_2]_f = 100$ μM, and $[TCP]_f = 300$ μM. All data were evaluated using Specfit Global Analysis System (Spectrum Software Associates) as pseudo-first-order reactions and fit with SVD analysis from one to three exponential curves where applicable. Kinetic data were baseline corrected using the Specfit autozero function.

Preparation of Reaction Intermediates by Freeze-Quench Methods. Rapid-freeze-quench experiments were performed with a BioLogic SFM 400 freeze-quench apparatus by mixing a 50 μM enzyme solution (final concentration) with a 10-fold excess of H_2O_2 solution in 100 mM potassium phosphate buffer (pH 5 and 7) at 25 °C. Reaction times were as follows: pH 5, 100 ms, 400 ms, 3.6 s, 36 s, and 60 s; and pH 7, 100 ms, 500 ms, 800 ms, 2 s, 12 s, and 60 s. A standard 4 mm outside diameter quartz EPR tube was connected to a Teflon funnel, and both the tube and the funnel were completely immersed in an isopentane bath at −110 °C. The reactions were quenched by spraying the mixtures into the cold isopentane, and the frozen material so obtained was packed at the bottom of the quartz tube using a packing rod equipped with a Teflon plunger. Samples were then transferred to a liquid nitrogen storage dewar until they were analyzed.

X-Band EPR Spectroscopy. EPR spectra were recorded with an X-band (9 GHz) Varian E-9 EPR spectrometer (Varian, El Palo, CA). A standard 3 mm × 4 mm quartz EPR tube was filled with a sample and placed into a quartz finger dewar insert filled with liquid nitrogen. The temperature of the samples was kept at 77 K for the duration of the data acquisition, which required periodic refilling of the dewar due to the evaporation of the liquid nitrogen during longer acquisition runs. The typical spectrometer settings were as follows: field sweep, 200 G; scan rate, 3.33 G/s; modulation frequency, 100 kHz; modulation amplitude, 4.0 G; and microwave power, 2 mW. The exact resonant frequency of each EPR experiment was measured by an EIP-578 (PhaseMatrix, San Jose, CA) in-line microwave frequency counter and is indicated in the figure captions. Typically, 20 and 200 individual scans were averaged to achieve sufficient signal to noise for the spectra obtained at short quench and long quench times, respectively.

RESULTS

UV−Visible Spectroscopic Studies of Ferric DHP in the Presence of TCP. The electronic absorption spectra of ferric metaquo DHP at pH 5 and 7 are presented in Figure 1. TCP exhibits absorbance maxima at 285 and 311 nm at pH 5.0 (Figure 1A) and pH 7.0 (Figure 1B), respectively. Although there is evidence for binding of substrate at an internal site in an X-ray crystal structure (*8*), there is also evidence for an external (*20, 21*) binding site. The spectra in Figure 1 show that TCP has a minimal effect on the heme spectra, and it is believed that TCP binds at an external binding site in the stopped-flow studies reported here.

Stopped-Flow UV−Visible Characterization of Compound ES in DHP. Single-mixing stopped-flow UV−visible spectroscopic methods were employed to detect DHP Compound ES. At pH 7, when a solution of ferric DHP [UV−visible spectrum, 407 (Soret), 504, 538, 635 nm] was rapidly mixed (2 ms) with H_2O_2, a transient species was observed (Figure 2 and Table 1), the spectral features of which [UV−visible, 420 (Soret), 545, 585 nm] we ascribe to a ferryl-containing DHP intermediate based upon previous characterization (*4, 7, 22*) and comparison to other known Fe(IV)−oxo species-containing hemoproteins (*11, 12*). As the ferryl intermediate of Compound ES is likely indistinguishable from that of Compound II by UV−visible spectroscopy, we assign this intermediate here as DHP Compound ES on the basis of these results and those of our EPR spectroscopic study (vide infra). Values of k_{obs} for formation of this new species were linearly dependent on H_2O_2 concentration (2.5−10-fold excess per heme), giving a bimolecular rate constant of (3.56 ± 0.02) × 10^4 M^{-1} s^{-1}. Under these conditions, and in the absence of substrate, DHP Compound ES decays to a stable species [UV−visible, 411 (Soret), 530, 564 nm; $k_{obs} = 0.0167 \pm 0.0003$ s^{-1}], which we have termed Compound RH.

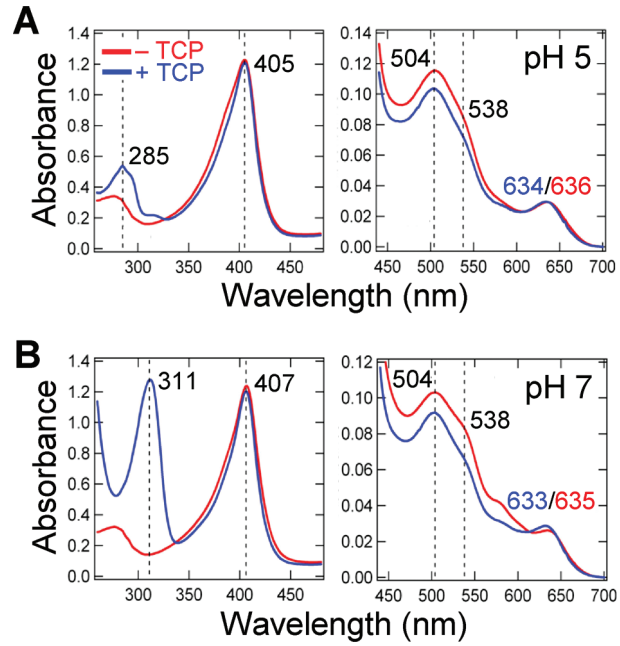

FIGURE 1: UV−visible spectra of ferric DHP (10 μM) in the presence (blue) and absence (red) of TCP (300 μM) at pH 5.0 (A) and pH 7.0 (B).

Similar reactivity is observed at pH 5. Ferric DHP [UV−visible, 405 (Soret), 504, 538, 636 nm] is converted to Compound ES [UV−visible, 419 (Soret), 545, 585 nm; $k_{obs} = (2.78 \pm 0.01) \times 10^4$ M^{-1} s^{-1}], which further decays to Compound RH [UV−visible, 410 (Soret), 530, 590 nm; $k_{obs} = 0.0701 \pm 0.0001$ s^{-1}] (Figure S1 of the Supporting Information). Hence, the rate of Compound RH formation is ~4 times greater at pH 5 than at pH 7.

Reaction of Preformed Compound ES with TCP Substrate. Stopped-flow UV−visible spectroscopy was employed to monitor the reaction between preformed DHP Compound ES and TCP. In a double-mixing experiment, 10 μM DHP was first reacted with a 10-fold excess of H_2O_2, allowed to incubate for 1.5 or 0.9 s, corresponding to the maximum accumulation of DHP Compound ES at pH 7 or 5, respectively, and then subsequently mixed with a 30-fold excess of TCP, which resulted in the regeneration of ferric (resting) DHP (Figure 3 and Figure S2 of the Supporting Information).

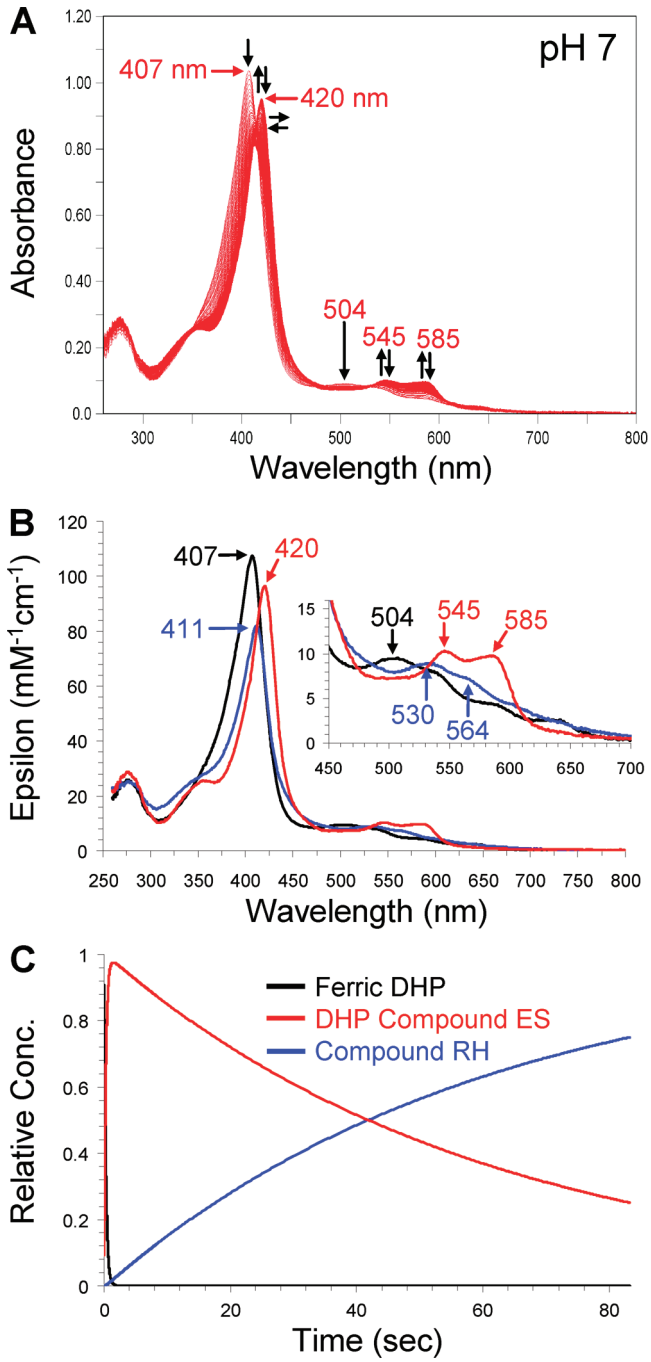

FIGURE 2: (A) Stopped-flow UV−visible spectroscopic monitoring of the reaction (900 scans, 85 s) between DHP (10 μM) and a 10-fold excess of H_2O_2 at pH 7.0. See Materials and Methods for details. (B) Calculated UV−visible spectra for resting (black), Compound ES (red), and Compound RH (blue) DHP are shown; the rapid-scanning data from panel A were compiled and fitted to a double-exponential reaction model using the Specfit global analysis program. (C) Relative concentration profile determined from the three-component fit used in panel B.

Under these conditions, nearly identical quantities of the DCQ product are formed at both pH values (Figure 4). However, it is interesting to note that at pH 5.0, the disappearance of Compound ES and the return of the enzyme to its resting state (8.47 ± 0.05 s^{-1}) are not directly coupled with product formation, which occurs subsequent to that process (0.13 ± 0.01 s^{-1}). On the other hand, at pH 7.0 the disappearance of DHP Compound ES (0.11 s^{-1}) is concomitant with the appearance of product (0.14 s^{-1}), although this observation does not prove that they are coupled. Nonenzymatic control experiments confirmed the necessity for DHP at both pH values, as no DCQ product was observed in the absence of the enzyme.

When the double-mixing experiments described above were repeated with longer incubation times that permitted Compound ES to completely decay to Compound RH prior to mixing with TCP, neither substrate loss (311 nm) nor product formation (275 nm) was observed during the 85 s time scale of these stopped-flow experiments. Specifically, at pH 5, Compound RH is nearly fully formed after 30 s (Figure S1c of the Supporting Information), with little to no Compound ES present, and neither the 30 nor 60 s incubation time exhibited product formation at this pH (Figure 4), indicating that Compound RH possesses a much lower catalytic activity than ferric DHP (vide infra). At pH 7, a 30 s incubation time results in a partial mixture of Compounds ES and RH being observed (Figure 2C), concomitant with partial substrate oxidation, whereas the 60 s incubation period led to no product formation, consistent with the nearly complete decay of Compound ES to Compound RH observed in the single-mixing experiments during this time frame. Thus, the extent of product formation is directly correlated with the amount of Compound ES present, strongly indicative that this intermediate is an active oxidant in DHP.

In Situ Compound ES Formation in the Presence of TCP. In contrast to the experiments described above in which preformed Compound ES was reacted with TCP, we employed double-mixing stopped-flow UV−visible spectroscopic methods to examine if preincubation of ferric DHP with TCP, followed by the addition of a 10-fold excess of H_2O_2, led to the formation of DCQ product (275 nm) via a transiently formed Compound ES intermediate. Under these conditions, the yield of DCQ product was nearly identical with that found for the reaction of fully preformed Compound ES with TCP (vide supra), at both pH 7 (Figure 5) and pH 5 (Figure S3 of the Supporting Information). When TCP was preincubated with DHP, there was no dependence on the delay time (1.5−60 s) prior to addition of H_2O_2 (Figure 6 and Figure S4 of the Supporting Information for pH 7 and 5, respectively). DCQ product formation had pseudo-first-order constants (k_{obs}) of 0.11 and 0.22 s^{-1} for pH 7.0 and 5.0, respectively. DCQ was also observed to be unstable under these conditions, undergoing side reaction(s) leading to its slow loss at longer time periods which were more apparent at pH 5 than at pH 7, but this chemistry was not further explored.

We also did note a pH-dependent difference with respect to the heme species observed. At pH 7.0, Compound ES [UV−visible, 420 (Soret), 545, 585 nm] is distinctly formed, with approximately the same rate [$k_{obs} = (3.11 \pm 0.02) \times 10^4$ M^{-1} s^{-1}] as when TCP was absent [$k_{obs} = (3.56 \pm 0.02) \times 10^4$ M^{-1} s^{-1}], and returns to the ferric state (UV−visible, 407, 504, 538, 578, 633 nm) with approximately the same rate ($k_{obs} = 0.12$ s^{-1}) as product formation (0.11 s^{-1}). At pH 5.0, no distinct Compound ES spectrum is observed upon reaction of hydrogen peroxide with DHP incubated in the presence of TCP; the UV−visible features [406 (Soret), 504, 538, and 635 nm] match those of the resting (ferric) enzyme, with the caveat that a minor broadening on the red side may be indicative of Compound ES formation and disappearance within the stopped-flow mixing time (2 ms).

Table 1: UV−Visible Spectroscopic Data and Kinetic Parameters for the Oxidized Intermediates of DHP

	pH 7		pH 5	
	λ_{max} (nm)	k_{obs} (M^{-1} s^{-1})	λ_{max} (nm)	k_{obs} (M^{-1} s^{-1})
ferric	407, 504, 538, 635	not applicable	405, 504, 538, 636	not applicable
Compound ES	420, 545, 585	$(3.56 \pm 0.02) \times 10^4$ M^{-1} s^{-1}	419, 545, 585	$(2.78 \pm 0.01) \times 10^4$ M^{-1} s^{-1}
Compound RH	411, 530, 564	0.0167 ± 0.0003 s^{-1}	410, 530, 590	0.0701 ± 0.0001 s^{-1}
Compound III	417, 542, 578	not determined	417, 542, 578	not determined

Characterization of Protein Radicals in DHP Compound ES. Rapid-freeze-quench methods were employed to stabilize intermediates of the reaction between DHP (final concentration of 50 μM) and a 10-fold excess of hydrogen peroxide at both pH 7 and 5 for consequent characterization by continuous wave (CW) EPR. X-Band CW EPR spectra of DHP samples recorded at pH 7.0 with various quench times are shown in Figure 7. The shapes of all the EPR spectra measured from the samples collected with quenching times of 500 ms, 800 ms, and 2 s were found to be identical, the only difference being in the signal intensities. The maximal concentration of the radical is observed over the period of Compound ES formation (Figure 2C). The position of the signal is characterized by an average g factor of 2.0058. The shape of the signal is best described by an anisotropic quintet. On the basis of the signal g factor and a partially resolved hyperfine structure with a peak-to-peak line width of ~21 G, this EPR signal was assigned to a tyrosyl radical (*23*). Samples with longer incubation times of 12 and 60 s have similar average g factors ($g \approx 2.005$) and the same peak-to-peak line width of 21 G; however, they do not exhibit resolved hyperfine structure and have much lower intensity [concomitant with the loss of the ferryl UV−visible spectrum in our component analysis (Figure 2C)].

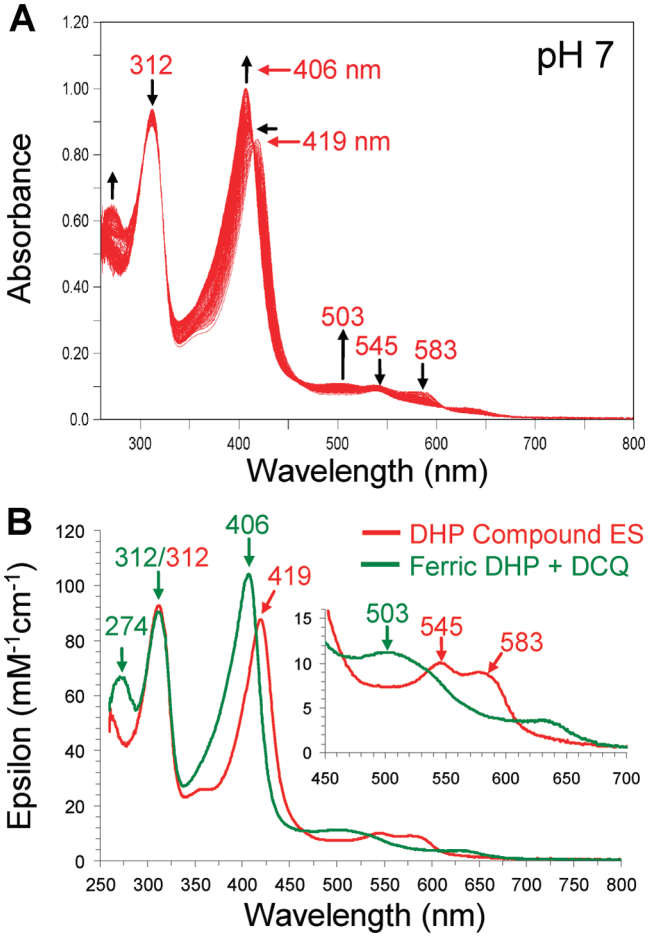

FIGURE 3: (A) Stopped-flow UV−visible spectroscopic monitoring of the double-mixing reaction (900 scans, 85 s) between preformed DHP Compound ES (10 μM) and TCP (300 μM) at pH 7. See Materials and Methods for details. (B) Calculated UV−visible spectra for both DHP Compound ES (red) and ferric DHP regenerated upon product formation (green); the rapid-scanning data from panel A were compiled and fitted to a single-exponential reaction model using the program Specfit.

The EPR spectrum of Compound ES was similarly recorded at various quench times at pH 5 (Figure 8). The spectrum is centered at $g = 2.0058$ and shows a partially resolved hyperfine splitting described as an "anisotropic septet" (*29*). A very weak shoulder is observed at $g = 2.035$ (Figure S5 of the Supporting Information) that could be an indication of the formation of a peroxyl radical since the samples were prepared under aerobic conditions (*30*), but the signal intensity is too low to warrant further speculation about its origin. At longer quench times when the component analysis indicates little to no remaining Compound ES by UV−visible spectroscopy (Figure S1c of the Supporting Information), the line shape of the EPR signal is drastically different, its signal intensity has dropped considerably, and the hyperfine splitting features are lost. Specifically, the signal has a very broad spectral feature in the $g \approx 2.04$ region and sharper features at $g = 2.0085$ and $g = 1.995$.

Unfortunately, the low g factor spectral resolution of these CW X-band experiments does not permit unambiguous identification of the radical species on the basis of magnetic parameters alone. This ambiguity could be resolved by high-field (95 GHz) EPR experiments coupled with mutagenesis studies that are planned for the near future.

Formation and Reactivity of Compound RH. As described above, in the absence of reducing substrate, a new, unique species of DHP, termed Compound RH to denote that is a reversible heme intermediate, is formed upon the decay of Compound ES. Compound RH was found to be robust to size-exclusion chromatography, protein concentration, and other sample preparation procedures. While its UV−visible features remained constant, we did observe that some protein

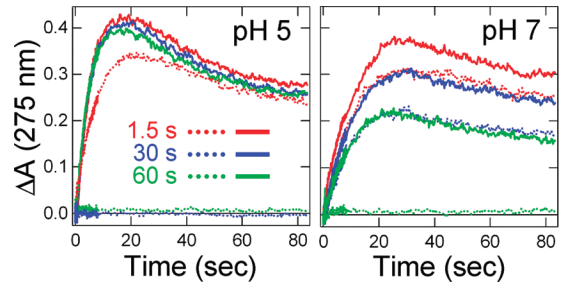

FIGURE 4: DCQ product formation (ΔA_{275}) as a function of pH for the following reaction conditions: preformed Compound ES with TCP (dotted lines) and TCP-preincubated DHP with H_2O_2 (solid lines). Both the aging time of Compound ES and the substrate preincubation period were varied (1.5, 30, and 60 s).

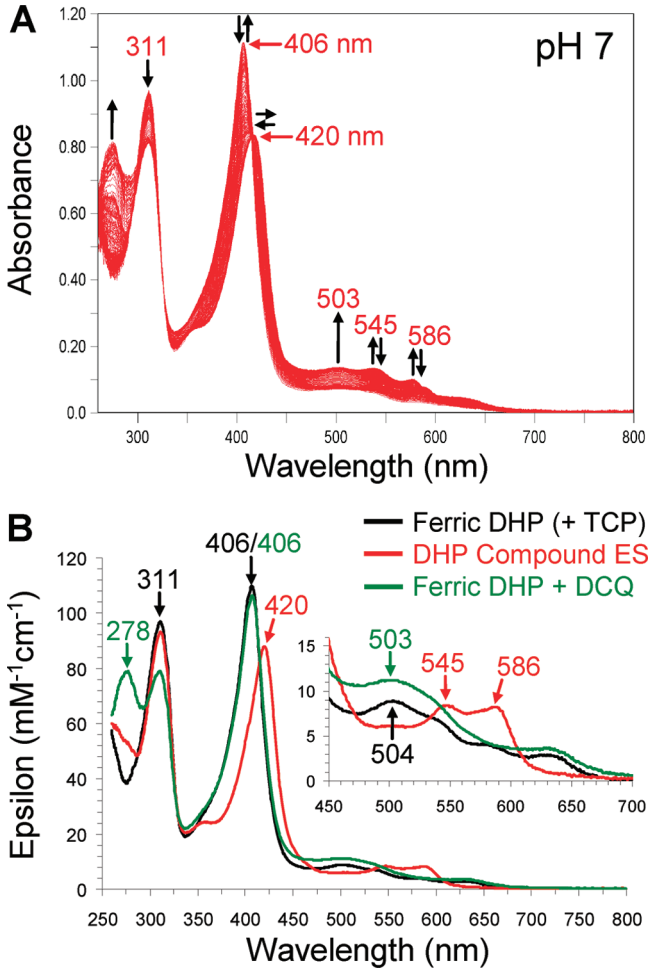

FIGURE 5: (A) Stopped-flow UV−visible spectroscopic monitoring of the double-mixing reaction (900 scans, 85 s) of ferric DHP (10 μM) preincubated with TCP (300 μM) for 1.5 s prior to its reaction with a 10-fold excess of H_2O_2 at pH 7. See Materials and Methods for details. (B) Calculated UV−visible spectra for ferric DHP incubated with TCP (black), the Compound ES intermediate formed (red), and ferric DHP regenerated upon product formation (green); the rapid-scanning data from panel A were compiled and fitted to a double-exponential reaction model using Specfit.

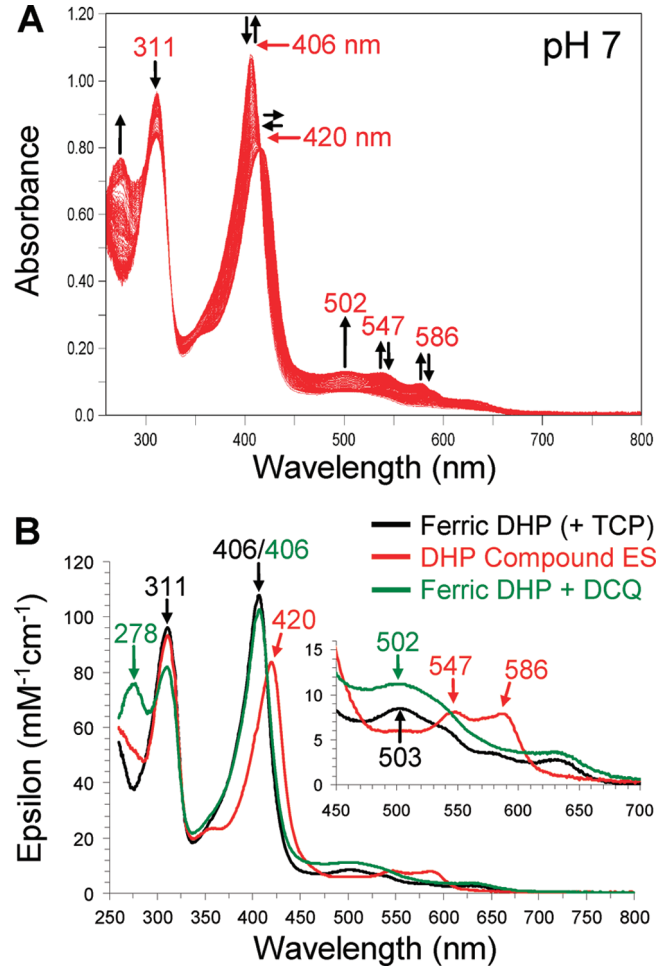

FIGURE 6: (A) Stopped-flow UV−visible spectroscopic monitoring of the double-mixing reaction (900 scans, 85 s) of ferric DHP (10 μM) preincubated with TCP (300 μM) for 60 s prior to its reaction with a 10-fold excess of H_2O_2 at pH 7. See Materials and Methods for details. (B) Calculated UV−visible spectra for ferric DHP incubated with TCP (black), the Compound ES intermediate formed (red), and ferric DHP regenerated upon product formation (green); the rapid-scanning data from panel A were compiled and fitted to a double-exponential reaction model using Specfit.

precipitation occurred when the long-term (several hours) room temperature stability of the Compound RH species was investigated. Addition of excess potassium cyanide (600 mM) to Compound RH resulted in a new UV−visible spectrum observed [421 (Soret), 545, 575 (sh) (data not shown)], consistent with the formation of a DHP ferricyanide adduct (*31*), providing further evidence that Compound RH is a single species.

To test the reactivity of the Compound RH species, single-mixing stopped-flow UV−visible spectroscopy was used to monitor the reaction between Compound RH (10 μM) and either a 10- or 100-fold molar excess of H_2O_2. In both cases, no reaction was observed [both pH 5 and 7 were investigated (data not shown)]. In spite of its inability to form high-valent iron−oxo intermediates, Compound RH still possesses attenuated levels of dehaloperoxidase activity, exhibiting a 6-fold lower reactivity with TCP as a substrate when compared to ferric DHP.

While Compound RH displays a lack of reactivity with H_2O_2 by stopped-flow UV−visible spectroscopy, it is readily reduced with sodium dithionite at either pH 5 or 7 to yield ferrous (deoxy) DHP [UV−visible, 432 (Soret), 557, 626 nm], which upon exposure to dioxygen led to formation of oxyferrous DHP [UV−visible, 417 (Soret), 542, 578 nm]. Further oxidation with potassium ferricyanide, followed by

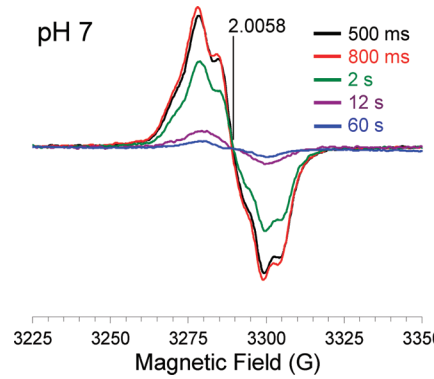

FIGURE 7: EPR spectra of the radical(s) in DHP Compound ES at pH 7. Rapid-freeze-quench samples were prepared from the reaction of DHP (final concentration of 50 μM) with a 10-fold molar excess of H_2O_2 at 25 °C and rapidly frozen in an isopentane slurry. Spectra were recorded at 77 K using the spectrometer settings described in Materials and Methods. The frequency of the experiments was 9.2330 GHz.

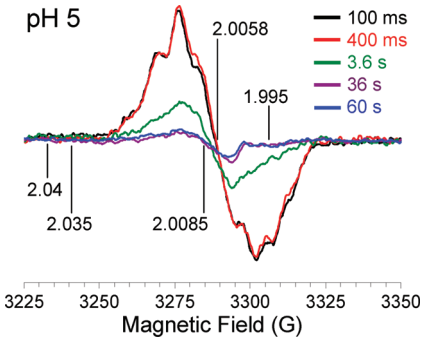

FIGURE 8: EPR spectra of the radical(s) in DHP Compound ES at pH 5. Rapid-freeze-quench samples were prepared from the reaction of DHP (final concentration of 50 μM) with a 10-fold molar excess of H_2O_2 at 25 °C and rapidly frozen in an isopentane slurry. Spectra were recorded at 77 K using the parameters described in Materials and Methods.

desalting, allowed for the reisolation of ferric DHP [UV−visible, 407 (Soret), 504, 538, 635 nm]. The activity of this "regenerated" ferric DHP was found to be nearly identical to that of as-isolated ferric DHP for TCP oxidation, suggesting that a pathway through Compound RH does not have any deleterious effect on dehaloperoxidase activity.

DISCUSSION

DHP has been shown to perform the net two-electron oxidation of phenol (X−A−OH + H_2O_2 → O=A=O + HX + H_2O) to yield the corresponding quinone, consistent with the reactive species being a two-electron-oxidized intermediate such as Compound I or Compound ES (*10*−*12*). However, the reaction of DHP with its physiological oxidant, H_2O_2, yields what had been characterized to date as Compound II, which is formally a one-electron-oxidized heme center. Thus, the question of how DHP oxidizes its phenol substrates by two electrons when it has been shown to only form a one-electron-oxidized intermediate needs to be addressed. This study provides further characterization of the intermediate formed from the reaction of ferric dehaloperoxidase with hydrogen peroxide, which suggests that this species is similar to the two-electron-oxidized Compound ES of CcP.

We employed stopped-flow UV−visible spectroscopic methods to monitor the reaction of ferric DHP with its physiological oxidant, H_2O_2. The first intermediate observed had spectral features which unequivocally match those for a ferryl-containing species lacking a porphyrin π-cation radical, such as Compound ES or Compound II. This implies either that Compound I is not formed by this reaction or more likely that it is formed transiently but undergoes rapid reduction to the observed Compound ES intermediate (vide infra). Interestingly, in the absence of a reducing substrate, the Compound ES intermediate was found to be unstable and converted to a new, stable species which we have termed Compound RH on the basis of the fact that it is a reversibly formed heme intermediate (RH, reversible heme). In the presence of substrate, however, Compound ES returned to the resting state, concomitant with formation of the quinone product. We examined this reaction with TCP using both preformed and in situ-generated Compound ES, and in both cases, the amount and rate of DCQ product generated were identical and independent of pH. The implication is that Compound ES is likely the actual species which is catalyzing TCP oxidation, rather than Compound I. If this were not the case, then one might expect different results between the amount and rate of product formation for in situ versus preformed Compound ES reactions. While this does not absolutely preclude a transiently formed Compound I species from oxidizing TCP, it strongly suggests that Compound ES is the active oxidant. Dichloroquinone product formation may result from either a single two-electron oxidation of the trichlorophenol substrate by Compound ES or two sequential one-electron oxidations, both pathways being indistinguishable under the multiple-turnover conditions examined in this study.

Stopped-flow UV−visible and rapid-freeze-quench EPR spectroscopic studies were employed to follow the formation of the high-valent iron(IV)−oxo and protein radical species, respectively, for the reaction of DHP with H_2O_2 leading to Compound ES. The UV−visible spectroscopic data indicate the direct formation of a classical ferryl-containing species, similar to that formed in HRP and Mb. Moreover, a recent ENDOR study by Hoffman and co-workers (*32*) supports the assignment as Fe(IV)=O, and not the protonated analogue Fe(IV)−OH (as in chloroperoxidase). The lack of an observable Compound I species suggested the presence of an endogenous reducing agent. As the crystal structure of DHP does not show any other redox capable cofactor (e.g., flavin, another metal center, etc.), we investigated by RFQ-CW-EPR spectroscopy whether a protein side chain could be responsible for the rapid reduction of a transiently formed Compound I species to the observed Compound ES intermediate, resulting in the formation of a protein radical. Indeed, we have identified the presence of a protein radical whose maximal concentration is observed over the period of Compound ES formation identified from UV−visible spectroscopy. As a result, we present here for the first time clear evidence of DHP Compound ES as a two-electron-oxidized intermediate, with one oxidation equivalent centered on the ferryl moiety and the second oxidation equivalent located on a protein side chain as a radical. Thus, DHP Compound ES bears a strong resemblance to CcP Compound ES, which has been extensively studied and shown to possess both a ferryl heme center and a radical on Trp^{191}.

Analysis of the signal *g* factor and the partially resolved hyperfine structure present in our EPR data, with a peak-to-peak line width of ~21 G, suggests that the radical in DHP Compound ES likely resides on a tyrosine residue initially (*23*). The longer incubation times of 12 and 60 s exhibit a similar average *g* factor ($g \approx 2.005$) and the same peak-to-peak line width of 21 G; however, they do not show resolved hyperfine structure and have much lower intensity [concomitant with the loss of the ferryl UV−visible spectrum in our component analysis (Figure 2C)]. Thus, it is difficult to comment extensively on the origin of these signals observed at later times. These spectra could be attributed to a different Tyr-based radical than the one initially observed, or the signal could also be an admixture of Tyr- and Trp-based radicals (*24*). Another option to consider is a radical originating from a cysteine residue, which is usually characterized by high *g* factor anisotropy that would be resolved in the X-band spectra (*25*−*27*). Although Cys-based radicals have been accepted as intermediates in metalloprotein cycles, they are not commonly observed by freeze-quench EPR

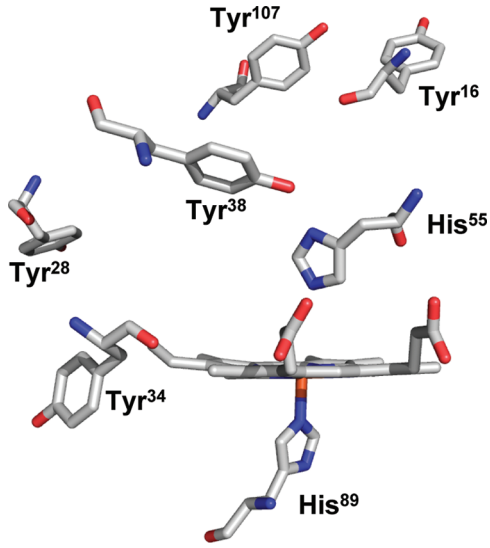

FIGURE 9: Active site of DHP showing all tyrosine residues present in the enzyme. The proximal and distal histidines, His^{89} and His^{55}, respectively, are provided for orientation. Coordinates (2QFK) were obtained from the Protein Data Bank and displayed using Pymol.

spectroscopy. However, Cys-based radicals should not be completely ruled out as intermediates at the quenching times of 12 and 60 s as they have been shown to form in human Mb under similar conditions (*28*).

Of the five tyrosine residues which DHP possesses [Tyr^{16}, Tyr^{28}, Tyr^{34}, Tyr^{38}, and Tyr^{107} (Figure 9)], only two are reasonably close to the heme prosthetic group to be considered likely candidates for reducing Compound I initially, Tyr^{34} and Tyr^{38}; the closest contact between Tyr^{34} and the heme edge is 5.56 Å (Tyr Cγ), whereas Tyr^{38} is 7.54 Å distant (phenolic oxygen). The three remaining tyrosine residues are more than 10 Å (Tyr^{28}) or 15 Å (Tyr^{16} and Tyr^{107}) from the heme edge. Furthermore, the closest heme edge to Trp^{120} (10.53 Å) and Cys^{73} (16.29 Å) contacts are similarly distant, making them unlikely candidates for the residues responsible for the initial reduction of the transiently formed Compound I intermediate. Thus, on the basis of both the available structural studies of DHP and our spectroscopic analysis presented here, we suggest that the initial site of radical formation in DHP Compound ES is either Tyr^{34} or Tyr^{38}.

While the definitive identification of the specific residue that gives rise to the initial protein radical in DHP Compound ES will be the subject of future high-field EPR investigations coupled with mutagenesis studies, the time-dependent changes observed in the protein radical signal suggest either a change in the local electronic structure of the radical or a migration of the radical out of the active site to other redox active protein side chains upon decay of Compound ES. This latter conjecture is interesting, given that the reaction of sperm whale Mb with hydrogen peroxide yields covalent dimers that arise from the coupling of surface tyrosyl radicals (Tyr^{151}), which results from a radical migration out of the Mb active site (*33*). Similarly, it has been demonstrated that human Mb also forms a covalent dimer (*34*), but through surface cysteines (Cys^{110}) forming a disulfide link, consistent with our putative radical observed at long quench times at pH 5 possessing a similar radical migration pathway, with surface radicals leading to the oxidation of TCP that binds to DHP through a hypothesized external binding pocket. This would not be unlike that of CcP, whose initial Trp^{191} radical in Compound ES leads to a radical migration which is ultimately responsible for oxidizing substrate (cytochrome *c*) at the surface of the peroxidase (protein−protein interface) (*35*). Thus, as CcP may have evolved from traditional (heme edge electron transfer) peroxidases an external binding interface for oxidizing cytochrome *c*, DHP may also similarly have evolved from Mb an external binding pocket for oxidizing trihalophenols. In accord with this hypothesis, tyrosine has been proposed to play a role in the peroxidase mechanism of Mb (*36*). This hypothesis will be particularly interesting if our supposition is that Tyr^{34} is the site of the radical in DHP Compound ES, as this residue is located at the surface of DHP yet is also in the proximity of the heme (Figure 9), and thus could serve as a redox conduit between the hypothesized external binding pocket and the active site.

From the initial observation in the X-ray crystal structure that 4-iodophenol (4IP) binds at an internal site in the distal pocket of DHP (*8*), the possibility of substrate binding to both internal and external binding pockets has been investigated with a number of techniques, including Fourier transform infrared (FTIR) (*20*), electron paramagnetic resonance (EPR) (*37*), nuclear magnetic resonance (NMR) (*21*), and resonance Raman experiments (Thompson and S. Franzen, unpublished results). Solution studies (*21*) and cryogenic studies (*20, 37*) have been carried out using 2,4,6-trifluorophenol (TFP) as a model of the native substrate 2,4,6-tribromophenol (TBP), which is relatively insoluble. EPR and HYSCORE experiments (*37*) are consistent with a change from six-coordinate high-spin to five-coordinate high-spin upon TFP binding at pH 6.0. TFP was used in those experiments because of its relatively high solubility, which facilitates detection under the conditions of the EPR experiment (4 K). FTIR experiments conducted on the carbonmonoxy form of DHP (DHP−CO) at cryogenic temperature (*20*) show that there is a large effect of TFP binding on the CO stretching frequency and rebinding kinetics at pH 5.5, but not at pH 7.0. However, near ambient temperature and physiological pH, TFP does not bind to DHP−CO (*20*). On the basis of the binding of 4IP in the distal pocket of DHP in the X-ray crystal structure, one hypothesis is that TFP is bound in the distal pocket of DHP−CO at low pH and at low temperatures. Hyperfine ^{1}H NMR experiments show that 4-bromophenol (4BP) and 2,4-dichlorophenol (DCP) interact with the metcyano form (DHP−CN) at ambient temperature through changes in the position of the internal heme edge Phe^{97} residue and the 3-CH_3 heme methyl (*21*). TFP does not produce these changes at ambient temperature, but there are shifts in ^{19}F resonances of the substrate when it interacts with DHP, which can be detected by ^{19}F NMR. From these data, one can further hypothesize that there is an external binding site (*21*) as well as the internal binding site observed by X-ray crystallography (*8*). Further confirmation can be found in resonance Raman experiments on 4IP and 4BP, which also show a change in core size marker modes when substrate binds (S. Franzen and Thompson, unpublished results). These experiments confirm that there is a change from six-coordinate high-spin in the resting metaquo form of DHP to five-coordinate high-spin when 4IP and 4BP bind. Thus, while 4IP and 4BP appear to bind inside the distal

Scheme 2: Proposed Catalytic Cycle for Dehaloperoxidase

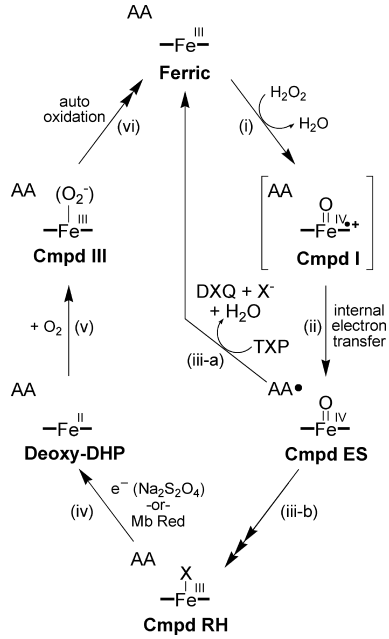

pocket, there are several observations that suggest that the external binding pocket is the active site.

In the absence of substrate, we observed that DHP Compound ES forms a new, stable species, termed Compound RH, which is unreactive toward H_2O_2 and, as a consequence, possesses attenuated levels of dehaloperoxidase activity. While peroxidase inactivation is a known phenomenon in HRP or CcP, where heme bleaching is the primary culprit (*38*), Compound RH is still active and can reversibly return to the deoxy ferrous state under mild reduction conditions. Furthermore, Compound RH has not been reported in myoglobin or hemoglobin previously, and is therefore unique to DHP (*33, 39*−*42*). Thus, as it is not found in either the monofunctional peroxidases or the O_2 transport globins, DHP Compound RH represents a novel species which may be a result of the bifunctional nature of DHP: the inactivated (dehalo)peroxidase can be regenerated back to an active oxygen transport protein via a reduction pathway that is specific for globins, but not peroxidases. When DHP is functioning as a peroxidase, its inactivation is necessary to prevent nonspecific oxidation of other metabolites from occurring when trihalophenol substrate is absent. However, while heme bleaching is a normal route for peroxidase inactivation, this could be metabolically costly for DHP, given that it is the hemoglobin in *A. ornata*. Thus, formation of Compound RH allows dehaloperoxidase to be inactivated without sacrificing the protein to heme bleaching while at the same time allowing for its functional switch back to an oxygen transport protein upon reduction. While the exact nature of the Compound RH species will require further study, it nevertheless represents an interesting and novel observation in this study.

A catalytic cycle can be proposed on the basis of the reversible formation of Compound RH. The catalytic cycle shown in Scheme 2 confers "hydrogen peroxide reductase" activity to dehaloperoxidase. The use of reducing agents to scavenge reactive oxygen species enzymatically is not unprecedented, with members of the peroxiredoxin family (Prx, also termed the thioredoxin peroxidases and alkylhydroperoxide-reductase-C22 proteins) and superoxide reductase (SOR) being perhaps the most well-known examples for H_2O_2 and superoxide reduction, respectively (*43, 44*). While disproportionation of H_2O_2 may be preferable over its reduction from a metabolic viewpoint, DHP does not exhibit significant catalase activity, although myoglobin has been shown to consume (noncatalytic) up to 8 equiv of H_2O_2 (*33, 41, 42*). Overall, should a partner reductase similar to Mb reductase be identified for DHP, the door for DHP to be considered a trifunctional protein capable of peroxidase, O_2 transport, and H_2O_2 scavenging activities would be opened.

On the basis of the results obtained from these stopped-flow UV−visible and RFQ-EPR spectroscopic experiments, and through modification of previously established mechanisms for the general function of peroxidases (*45*), we propose the following catalytic cycle for the in vitro peroxide-dependent oxidation of ferric DHP from *A. ornata* in the presence and absence of trihalophenol (Scheme 2). Ferric DHP reacts with 1 equiv of H_2O_2, transiently forming Compound I (step i), which then undergoes rapid endogenous electron transfer to generate the observed Compound ES intermediate and protein radical (step ii). A bifurcation in the mechanism occurs which is dependent upon substrate. In the presence of trihalophenol, DHP Compound ES is reduced by two electrons, thereby regenerating the ferric state of the enzyme, and forming the dihaloquinone product (step iii-a). In the absence of substrate, however, Compound RH is formed (iii-b) by a not-yet-understood process and can subsequently be reduced to the ferrous enzyme (iv) and bind dioxygen to form the oxyferrous intermediate (v). Autoxidation of oxyferrous DHP leads to the formation of the ferric enzyme (vi). The existence, and by extension identity, of a possible sixth ligand in Compound RH is unknown at this time, and this ambiguity is represented by the bound X in Scheme 2. We tentatively assign the oxidation state of Compound RH as a ferric heme on the basis of the evidence that (i) Compound RH exhibits a "ferric-like" heme spectrum that matches neither the ferryl nor the ferrous spectra of DHP (Table 1), (ii) Compound RH forms from the decay of an iron(IV)−oxo species, which for most heme proteins yields a ferric enzyme, and (iii) Compound RH can be reduced to the ferrous enzyme, implying that it does not start as a ferrous heme. Further studies will be necessary to definitively assign the oxidation state of the heme in Compound RH.

CONCLUSION

This study addresses a number of key questions pertaining to the nature and catalytic competency of the Compound ES intermediate in DHP. Our spectroscopic and biochemical characterization of DHP Compound ES suggests that this species is similar to the two-electron-oxidized Compound ES of CcP in that it possesses both a ferryl heme center and a protein radical. Furthermore, our results are consistent with Compound ES being an active species responsible for trihalophenol oxidation, as opposed to Compound I. The data support the hypothesis that there is an external substrate binding pocket in DHP, in which case the data reported here indicate that there may be a radical migration pathway in DHP analogous to that in CcP. A peroxidase-attenuated species unique to DHP, namely Compound RH, was also

identified, and a role for its formation as a protective species against unwanted oxidation chemistry was hypothesized. As Compound RH is unreactive toward further oxidation, it was found that reduction of Compound RH regenerates oxyferrous DHP, and this suggests that the recovery of the oxygen transport function from an attenuated peroxidase species via reduction (possibly globin reductase) is a consequence of the bifunctional nature of this protein and may represent the chemical process that links the oxygen transport and peroxidase activities in dehaloperoxidase.

SUPPORTING INFORMATION AVAILABLE

Molar absorbances for 2,4,6-trichlorophenol at pH 5, 6, 7, and 7.5 (Table S1), stopped-flow UV−visible spectroscopic monitoring of the reaction between DHP and a 10-fold molar excess of H_2O_2 at pH 5.0 (Figure S1), stopped-flow UV−visible spectroscopic monitoring of the double-mixing reaction between preformed DHP Compound ES and TCP at pH 5 (Figure S2), stopped-flow UV−visible spectroscopic monitoring of the double-mixing reaction of ferric DHP preincubated with TCP for 1.5 s prior to its reaction with H_2O_2 at pH 5 (Figure S3), stopped-flow UV−visible spectroscopic monitoring of the double-mixing reaction of ferric DHP preincubated with TCP for 60 s prior to its reaction with H_2O_2 at pH 5 (Figure S4), and rapid-freeze-quench data at pH 5 (Figure S5). This material is available free of charge via the Internet at http://pubs.acs.org.

REFERENCES

1. Weber, R. E., Magnum, C. P., Steinman, H., Bonaventura, C., Sullivan, B., and Bonaventura, J. (1977) Hemoglobins of two terebellid polychaetes: *Enoplobranchus sanuigneus* and *Amphitire ornata*. *Comp. Biochem. Phys. 56A*, 179–187.
2. Chen, Y. P., Woodin, S. A., Lincoln, D. E., and Lovell, C. R. (1996) An unusual dehalogenating peroxidase from the marine terebellid ploychaete *Amphitrite ornata*. *J. Biol. Chem. 271*, 4609–4612.
3. Osborne, R. L., Coggins, M. K., Walla, M., and Dawson, J. H. (2007) Horse heart myoglobin catalyzes the H_2O_2-dependent oxidative dehalogenation of chlorophenols to DNA-binding radicals and quinones. *Biochemistry 46*, 9823–9829.
4. Belyea, J., Gilvey, L. B., Davis, M. F., Godek, M., Sit, T. L., Lommel, S. A., and Franzen, S. (2005) Enzyme function of the globin dehaloperoxidase from *Amphitrite ornata* is activated by substrate binding. *Biochemistry 44*, 15637–15644.
5. Hardison, R. (1998) Hemoglobins from bacteria to man: Evolution of different patterns of gene expression. *J. Exp. Biol. 201*, 1099–1117.
6. Bailly, X., Chabasse, C., Hourdez, S., Dewilde, S., Martial, S., Moens, L., and Zal, F. (2007) Globin gene family evolution and functional diversification in annelids. *FEBS J. 274*, 2641–2652.
7. Franzen, S., Gilvey, L. B., and Belyea, J. L. (2007) The pH dependence of the activity of dehaloperoxidase from *Amphitrite ornata*. *Biochim. Biophys. Acta 1774*, 121–130.
8. LaCount, M. W., Zhang, E. L., Chen, Y. P., Han, K. P., Whitton, M. M., Lincoln, D. E., Woodin, S. A., and Lebioda, L. (2000) The crystal structure and amino acid sequence of dehaloperoxidase from *Amphitrite ornata* indicate common ancestry with globins. *J. Biol. Chem. 275*, 18712–18716.
9. Poulos, T. L., and Kraut, J. (1980) The structure of cytochrome c peroxidase at 2.5 Å resolution. *J. Biol. Chem. 255*, 575–580.
10. Akita, M., Tsutsumi, D., Kobayashi, M., and Kise, H. (2001) Structural change and catalytic activity of horseradish peroxidase in oxidative polymerization of phenol. *Biosci., Biotechnol., Biochem. 65*, 1581–1588.
11. Laurenti, E., Ghibaudi, E., Todaro, G., and Ferrari, R. P. (2002) Enzymatic degradation of 2,6-dichlorophenol by horseradish peroxidase: UV-visible and mass spectrophotometric characterization of the reaction products. *J. Inorg. Biochem. 92*, 75–81.
12. Laurenti, E., Ghibaudi, E., Ardissone, S., and Ferrari, R. P. (2003) Oxidation of 2,4-dichlorophenol catalyzed by horseradish peroxidase: Characterization of the reaction mechanism by UV-visible spectroscopy and mass spectrometry. *J. Inorg. Biochem. 95*, 171–176.
13. Raven, E. L. (2000) Peroxidase-Catalyzed Oxidation of Ascorbate. In *Subcellular Chemistry, Volume 35: Enzyme-Catalyzed Electron and Radical Transfer* (Holzenburg, A., and Scrutton, N., Eds.) pp 317−349, Kluwer Academic/Plenum Publishers, New York.
14. Neely, W. B. (1984) An Analysis of Aquatic Toxicity Data: Water Solubility and Acute Lc50 Fish Data. *Chemosphere 13*, 813–819.
15. Dannenfelser, R. M., and Yalkowsky, S. H. (1991) Data-Base of Aqueous Solubility for Organic Nonelectrolytes. *Sci. Total Environ. 109*, 625–628.
16. Falk, J. E. (1964) Haems. I. Determination as pyridine hemochromes. *Porphyrins and Metalloporphyrins: Their General, Physical, and Coordination Chemistry and Laboratory Methods*, pp 181−188, Elsevier Publishing, New York.
17. Fuhrhop, J. H., and Smith, K. M. (1975) Laboratory Methods. In *Porphyrins and Metalloporphyrins* (Smith, K. M., Ed.) pp 804−807, Elsevier Publishing, New York.
18. Beers, R. F., Jr., and Sizer, I. W. (1952) A spectrophotometric method for measuring the breakdown of hydrogen peroxide by catalase. *J. Biol. Chem. 195*, 133–140.
19. Osborne, R. L., Taylor, L. O., Han, K. P., Ely, B., and Dawson, J. H. (2004) *Amphitrite ornata* dehaloperoxidase: Enhanced activity for the catalytically active globin using MCPBA. *Biochem. Biophys. Res. Commun. 324*, 1194–1198.
20. Nienhaus, K., Deng, P. C., Belyea, J., Franzen, S., and Nienhaus, G. U. (2006) Spectroscopic study of substrate binding to the carbonmonoxy form of dehaloperoxidase from *Amphitrite ornata*. *J. Phys. Chem. B 110*, 13264–13276.
21. Davis, M. F., Gracz, H., Vendeix, F. A. P., Gilvey, L. B., Somasundaram, A., Decatur, S. M., and Franzen, S. (2009) Different Binding Modes of Mono-, Di- and Trihalogenated Phenols to the Hemoglobin Dehaloperoxidase from *Amphitrite ornata*. *Biochemistry* . (submitted for publication).
22. Franzen, S., Chaudhary, C., Belyea, J., Gilvey, L., Davis, M. F., Sit, T. L., and Lommel, S. A. (2006) Proximal cavity, distal histidine and substrate hydrogen-bonding mutations modulate the activity of *Amphitrite ornata* dehaloperoxidase. *Biochemistry 45*, 9085–9094.
23. Svistunenko, D. A., and Cooper, C. E. (2004) A new method of identifying the site of tyrosyl radicals in proteins. *Biophys. J. 87*, 582–595.
24. Svistunenko, D. A., Dunne, J., Fryer, M., Nicholls, P., Reeder, B. J., Wilson, M. T., Bigotti, M. G., Cutruzzola, F., and Cooper, C. E. (2002) Comparative study of tyrosine radicals in hemoglobin and myoglobins treated with hydrogen peroxide. *Biophys. J. 83*, 2845–2855.
25. Lawrence, C. C., Bennati, M., Obias, H. V., Bar, G., Griffin, R. G., and Stubbe, J. (1999) High-field EPR detection of a disulfide radical anion in the reduction of cytidine 5′-diphosphate by the E441Q R1 mutant of *Escherichia coli* ribonucleotide reductase. *Proc. Natl. Acad. Sci. U.S.A. 96*, 8979–8984.
26. Hoffman, M. Z., and Hayon, E. (1972) One-Electron Reduction of Disulfide Linkage in Aqueous-Solution: Formation, Protonation, and Decay Kinetics of $RSSR^-$ Radical. *J. Am. Chem. Soc. 94*, 7950–7957.
27. Chan, P. C., and Bielski, B. H. J. (1973) Pulse-Radiolysis Study of Optical-Absorption and Kinetic Properties of Dithiothreitol Free-Radical. *J. Am. Chem. Soc. 95*, 5504–5508.
28. Witting, P. K., Douglas, D. J., and Mauk, A. G. (2000) Reaction of human myoglobin and H_2O_2: Involvement of a thiyl radical produced at cysteine 110. *J. Biol. Chem. 275*, 20391–20398.
29. Svistunenko, D. A. (2005) Reaction of haem containing proteins and enzymes with hydroperoxides: The radical view. *Biochim. Biophys. Acta 1707*, 127–155.
30. Lund, M. N., Luxford, C., Skibsted, L. H., and Davies, M. J. (2008) Oxidation of myosin by haem proteins generates myosin radicals and protein cross-links. *Biochem. J. 410*, 565–574.
31. Roach, M. P., Chen, Y. P., Woodin, S. A., Lincoln, D. E., and Dawson, J. H. (1997) *Notomastus lobatus* chloroperoxidase and *Amphitrite ornata* dehaloperoxidase both contain histidine as their proximal heme iron ligand. *Biochemistry 36*, 2197–2202.
32. Davydov, R., Osborne, R. L., Kim, S. H., Dawson, J. H., and Hoffman, B. M. (2008) EPR and ENDOR studies of cryoreduced compounds II of peroxidases and myoglobin. Proton-coupled electron transfer and protonation status of ferryl. *Biochemistry 47*, 5147–5155.

33. Fenwick, C. W., and English, A. M. (1996) Trapping and LC-MS identification of protein radicals formed in the horse heart met-myoglobin-H_2O_2 reaction. *J. Am. Chem. Soc. 118*, 12236–12237.
34. Hirota, S., Azuma, K., Fukuba, M., Kuroiwa, S., and Funasaki, N. (2005) Heme reduction by intramolecular electron transfer in cysteine mutant myoglobin under carbon monoxide atmosphere. *Biochemistry 44*, 10322–10327.
35. Smith, A. T., and Veitch, N. C. (1998) Substrate binding and catalysis in heme peroxidases. *Curr. Opin. Chem. Biol. 2*, 269–278.
36. Witting, P. K., Mauk, A. G., and Lay, P. A. (2002) Role of tyrosine-103 in myoglobin peroxidase activity: Kinetic and steady-state studies on the reaction of wild-type and variant recombinant human myoglobins with H_2O_2. *Biochemistry 41*, 11495–11503.
37. Smirnova, T. I., Weber, R. T., Davis, M. F., and Franzen, S. (2008) Substrate binding triggers a switch in the iron coordination in dehaloperoxidase from *Amphitrite ornata*: HYSCORE experiments. *J. Am. Chem. Soc. 130*, 2128–2129.
38. Gajhede, M. (2001) Horseradish Peroxidase. In *Handbook of Metalloprotein* (Messerschmidt, A., Huber, R., Poulos, T. L., and Weighardt, K., Eds.) pp 195−210, John Wiley & Sons, Inc., Chichester, U.K.
39. Keilin, D., and Hartree, E. F. (1950) Reaction of Methaemoglobin with Hydrogen Peroxide. *Nature 166*, 513–514.
40. George, P., and Irvine, D. H. (1951) Reaction of Metmyoglobin with Hydrogen Peroxide. *Nature 168*, 164–165.
41. Giulivi, C., and Cadenas, E. (1998) Heme protein radicals: Formation, fate, and biological consequences. *Free Radical Biol. Med. 24*, 269–279.
42. Alayash, A. I., Ryan, B. A. B., Eich, R. F., Olson, J. S., and Cashon, R. E. (1999) Reactions of sperm whale myoglobin with hydrogen peroxide: Effects of distal pocket mutations on the formation and stability of the ferryl intermediate. *J. Biol. Chem. 274*, 2029–2037.
43. Wood, Z. A., Schroder, E., Harris, J. R., and Poole, L. B. (2003) Structure, mechanism and regulation of peroxiredoxins. *Trends Biochem. Sci. 28*, 32–40.
44. Niviere, V., and Fontecave, M. (2004) Discovery of superoxide reductase: An historical perspective. *J. Biol. Inorg. Chem. 9*, 119–123.
45. Dunford, H. B. (1999) *Heme Peroxidases*, Wiley-VCH, New York (and references cited therein).

BI801916J